Single- and double-electron capture probabilities in close sub-MeV collisions of He^{2+} on Ar and N_2

I. Ben-Itzhak,* A. Mann, M. Meron,† and B. Rosner
Department of Physics, Technion, Haifa 32000, Israel
(Received 27 March 1989)

Single- and double-electron capture probabilities of 400–1000-keV He^{2+} projectiles in large-angle scattering on Ar and N_2 targets were studied. A classical model for these probabilities, based on the Bohr-Lindhard capture model, was developed for collisions at very small impact parameters with multielectron targets. The model takes into account post-collision relaxation processes when evaluating the double-electron capture probability.

I. INTRODUCTION

Single- and double-electron capture by a fast bare projectile has been studied experimentally[1–8] as well as theoretically.[8–11] Most of the work was done by measuring the total cross sections for these processes. More recently, work in which the impact-parameter dependence of capture probabilities became of great interest[12–18] as it enables us to gain a better understanding of the electron-transfer mechanism and a test ground for theories of charge exchange.

In the case of intermediate velocities close collisions (namely, those with closest approach distances smaller than the K-shell radius of the target atom and with velocities faster than the outer-shell electrons' orbital velocity and slower than the core electrons) charge exchange probabilities become almost independent of the impact parameter.[12–15] On the other hand, similar collisions at relatively higher velocities show structure in the differential capture cross sections.[16–18] This structure is due to the Thomas capture mechanism[19] which is negligible at the velocities of interest in this study.

The theoretical problem of how to evaluate the single-electron capture probability from a multielectron target is rather complicated because of the number of electrons involved. Double-electron capture is even more complicated as electron correlations may be important, and because double-electron capture into autoionizing states will be detected as single-electron capture. A classical model for electron capture was suggested by Bohr and Lindhard,[20,21] and modified by Knudsen *et al.*[22] to include a more realistic velocity distribution for the target electrons. Brandt[23] introduced an impact-parameter dependence into the Bohr-Lindhard model. In the collisions studied, the projectile velocity is faster than the target's outer-shell electrons' velocity and slower than the core electrons' velocity. For the core electrons the collision is approximately adiabatic and is well described by the molecular-orbital model suggested by Fano and Lichten.[24] The contributions from inner shells and outer shells can be treated separately for the systems studied, as shown by Meron *et al.*[25] Furthermore, electron capture from inner shells is negligible for the colliding systems of interest in this work.

In this paper we report the results of measurements of single- and double-capture probabilities by α particles, for very small impact parameters at intermediate velocities. A model for electron capture, which is based on the Bohr-Lindhard model, is developed and is in good agreement with the experimental results. Atomic units are used throughout this paper (unless units are specified).

II. EXPERIMENT

He^+ beams in the energy range of 0.4–1 MeV were generated by the Technion 1-MV Van de Graaff accelerator. The energy was defined to <2 keV using a 15° analyzing magnet. Two sets of defining slits were used to collimate the beam to less than 0.5 mm diameter at the entrance to the scattering chamber, with an angular width of at most 0.02°. A beam of He^{2+} was obtained from the singly charged beam using a gas stripper upstream of the analyzing magnet. A detailed description of the experimental system (presented in Fig. 1) and the experimental procedures was published in previous work.[13,25]

The differentially pumped gas target was located in the center of a 70-cm scattering chamber. A combination of two stages of differential pumping with small entrance and exit slits allowed us to maintain a pressure of $(0.5-1)\times10^{-3}$ Torr in the target cell while the pressure in the scattering chamber was kept below 3×10^{-6} Torr. The gases used were Ar and N_2. The target cell diameter was 10 mm.

The analysis and detection system was mounted as a rigid unit on a rotatable arm in the scattering chamber. This system included an adjustable slit, charge analyzing electrostatic deflector, and a 25-mm position-sensitive silicon detector. The scattering angle of the analyzed particles was defined to 0.05° by the entrance slit. The aperture of the electrostatic deflector was sufficient to spread the analyzed charge states across the whole width of the detector. Given the nominal position resolution of 0.2 mm this setup was capable of separating all the charge states of the projectile. In practice, however, the position resolution depends critically on the measurable energy of the particle, i.e., original energy minus energy loss in the detector's dead layer. For 0.4-MeV He ions the position

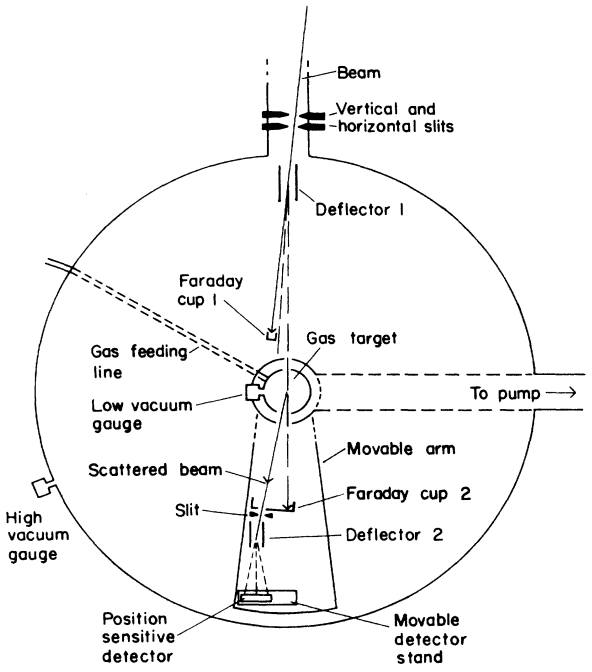

FIG. 1. The experimental system for measuring charge state distributions of scattered ions.

resolution was around 6 mm, just sufficient to resolve the three He charge states over the 25 mm length of the detector. That determined the lower energy limit of the experiment.

Throughout the measurement special care has been taken to ensure the purity of the incoming beam, and to avoid distortion of the results by slit scattering. For charged beams an additional electrostatic deflector upstream of the gas target was used in conjunction with a Faraday cup to measure the beam composition. In all cases the beam purity was found to be better than 99%.

In Fig. 2 we present the impact-parameter dependence of the probabilities for single- and double-electron capture by He^{2+} impinging on Ar target at 800 keV. The transformation from the laboratory scattering angle to impact parameter was done using an exponentially screened Coulomb potential.[25] It can be seen clearly that there is almost no dependence on the impact parameter once the K-shell radius is crossed. Similar results were obtained for all the systems studied in intermediate velocity collisions, 2–3.2 a.u. (100–250 keV/amu), i.e., the projectile velocity is larger than the orbital velocity of loosely bound electrons of the target and smaller than the orbital velocity of the tightly bound electrons.

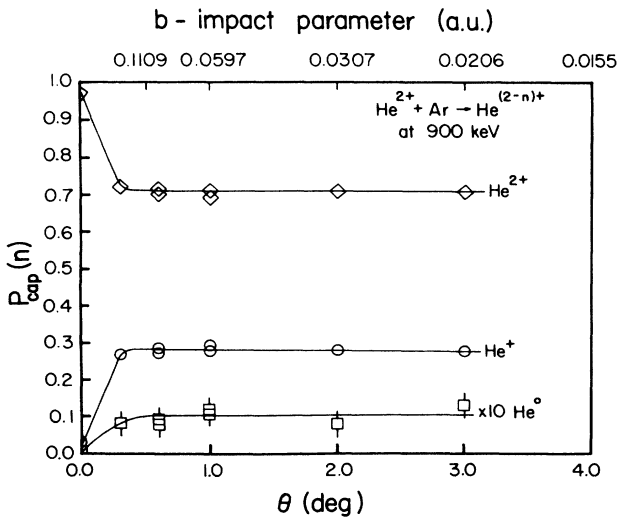

FIG. 2. Angular distribution of outgoing He charge states after a collision with an Ar atom, at 900 keV.

III. THEORY

A full quantum-mechanical treatment of the single-electron capture from a multielectron target in a fast close collision is still too complicated to be handled exactly. It is even more so for the double-electron capture for the same kind of collisions. Classical models such as the Bohr-Lindhard[20,21] model for ionization and capture, and classical trajectory Monte Carlo calculations[26,27] (CTMC) have some success. We will try to follow a similar approach and develop a simple model for the single- and double-electron capture probability, at zero impact parameter, from a multielectron target.

A. The Bohr-Lindhard model

Bohr and Lindhard[20,21] described electron capture by a fast projectile as a two-step process. First the electron is released from the target with a negligible velocity relative to the target, and close to the target nucleus. An electron can be released from the target when the projectile passes closely enough so that the force exerted by it on the electron overcomes the binding force of the electron in the target. This condition defines the release radius R_r by $q/R_r^2 = v^2/a$, i.e., $R_r = (qa/v^2)^{1/2}$, where q is the projectile's charge and a and v are the electron's orbital radius and velocity, respectively. Within the distance R_r around the projectile's trajectory all electrons can be captured. The release process takes time of the order of the orbital period, $\tau \sim a/v$. A released electron will be captured if its energy in the projectile rest frame is negative. The limiting condition for this defines a capture radius R_c, through

$$\frac{q}{R_c} = \frac{v_p^2}{2} , \tag{1}$$

where v_p is the projectile velocity. For fast collisions the Bohr-Lindhard model gives the capture cross section,

$$\sigma_c = 16\pi \frac{E_B q^3}{\nu v_p^7} , \tag{2}$$

where ν is an effective quantum number (in atomic units $a = \nu$; $\nu = 1$ for the $1s$ state), and E_B is the electron binding energy, related to v by $v = (2E_B)^{1/2}$.

B. The Brandt model

Following the Bohr-Lindhard approach Brandt[23] introduced an impact-parameter dependence into this model. The impact-parameter dependence is introduced by taking into account the different times spent by projectiles having different impact parameters in the vicinity of the released electron. The single-electron capture probability is given by

$$P(b)=\frac{2(R_c^2-b^2)^{1/2}}{\tau v_p} , \tag{3}$$

and the total capture cross section from a single-electron target is then

$$\sigma_c=\frac{64}{3}\pi\frac{E_B q^3}{\nu v_p^7} . \tag{4}$$

The total cross section is a factor of $\frac{4}{3}$ larger than the Bohr-Lindhard cross section. For multielectron targets Brandt uses the independent-electron approximation. The single-electron capture probability for zero impact parameter reduces to

$$P(b=0)=\frac{8E_B q}{\nu v_p^3} . \tag{5}$$

C. The "frozen target" model

Our aim is to calculate the electron capture probability for close collisions from a multielectron target. As the Bohr-Lindhard model is in good agreement with measured cross sections for single-electron capture in the energy regime of our interest, we will base our calculations on similar basic assumptions.

For fast close collisions with an impact parameter of the order of 0.01 a.u. and a small scattering angle ($<3°$), the projectile trajectory can be approximated by a straight line passing through the target nucleus, i.e., $b=0$ for the calculation.

In the intermediate energy regime, the projectile velocity is greater than the orbital velocity of the loosely bound electrons. For these slow electrons the number density,

$$\rho(r)=\sum_{n,l,m}|\psi_{n,l,m}(r)|^2 ,$$

is approximately constant during the collision. We represent the target electrons, available for capture, by the "frozen" target number density $\rho'(r)$. The fast electrons are tightly bound and are not released by the projectile-electron interaction so they cannot be captured in the Bohr-Lindhard model. Capture of these fast electrons is well described by the molecular-orbital (MO) model[24] and its contribution is negligible for the collision conditions studied in this work. We neglect the contribution to charge transfer of these tightly bound electrons. An electron is considered to be tightly bound in our model if its orbital velocity is greater than the projectile velocity. In our model of the target atom these electrons are represented by the number density confined in a sphere with radius R_F defined by $v_e(R_F)=v_p$. Now, using the Bohr model of the atom we can define an equivalent velocity of an electron at a distance r from the target nucleus

$$\frac{v_e^2}{r}=\frac{Z_{\text{eff}}(r)}{r^2} ; \tag{6}$$

using the definition of R_F and Eq. (6) we get

$$R_F=\frac{Z_{\text{eff}}(R_F)}{v_p^2} . \tag{7}$$

The effective charge Z_{eff} at a distance R_F from the target nucleus can be found by integrating the number density

$$Z_{\text{eff}}(r)=Z_T-4\pi\int_0^r\rho(r')r'^2dr' . \tag{8}$$

Now, R_F can be evaluated by solving numerically the equation that follows from Eq. (7) and Eq. (8)

$$R_F=\frac{1}{v_p^2}\left[Z_T-4\pi\int_0^{R_F}\rho(r')r'^2dr'\right] . \tag{9}$$

After subtracting the contribution of the tightly bound electrons from the electron number density $\rho(r)$, the remaining slow electrons described by the number density $\rho'(r)$ can be captured if their distance from the projectile is smaller than a capture radius R_c defined by the classical condition suggested by Bohr and Lindhard.[21] Thus electrons are captured if their total energy in the rest frame of the projectile is negative

$$0\geq E_{\text{total}}=\frac{v_p^2}{2}-|\mathcal{E}_T|-\frac{Z_p}{r'} , \tag{10}$$

where r' is the distance of closest approach of an electron to the projectile, and $|\mathcal{E}_T|$ is an average binding energy on the target. The maximum distance from the projectile in which electrons can be captured, i.e., the capture radius, is then

$$R_c=\frac{2Z_p}{v_p^2-2|\mathcal{E}_T|} . \tag{11}$$

For fast collisions $v_p^2/2\gg|\mathcal{E}_T|$ and the capture radius is independent of the target binding energy

$$R_c=\frac{2Z_p}{v_p^2} . \tag{12}$$

The capture radius defines a cylinder, with its axis $\hat{z}$ along the projectile velocity, in which electrons are captured. A schematic description of the collision is shown in Fig. 3. The probability for electron capture is then the integral along this cylinder of the number density $\rho'(r)$, i.e., the probability of a loosely bound electron to be within a distance R_c from the projectile path.

If more than one electron is captured during the collision, it is probable that some electrons will be ejected as Auger electrons as the projectile relaxes to its ground state. In the present experiment the charge state analysis of the projectiles was done ~ 30 nsec after the collision so that most states will decay to the ground state or to meta-

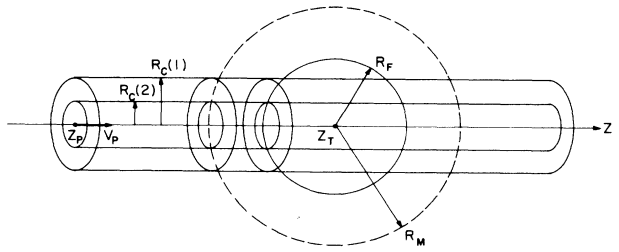

FIG. 3. A schematic view of the "frozen target" collision model. See text for further details.

stable states. The Auger decay mechanism is dominant for doubly excited He-like projectiles so that in most of the events where double capture was detected, one of the electrons was captured to the ground state. In order to represent this reduction in the final number of electrons captured by the projectile we assume that the capture process happens sequentially and the effective charge of the projectile is reduced after each electron capture. This reduction in the effective charge of the projectile will decrease the capture radius of the next electron relative to the previous electron capture radius. The capture radius for sequential capture of the nth electron is then (assuming complete screening by the captured electrons)

$$R_c(n)=\frac{2(Z_p-n+1)}{v_p^2-2|\mathcal{E}_T|} . \tag{13}$$

In order to calculate the single- and double-electron capture probabilities for $He^{2+}+Ar$ and $He^{2+}+N_2$ collisions, in which the probabilities are comparable to 1, we used a Poisson-like process. This was done to ascertain that the unitarity condition will be fulfilled. The target atom is divided into thin spherical shells of thickness dr, so that the probability of finding an electron within a shell is small and the probability of finding two electrons is negligible. Thus the electron capture probabilities are given by integrating the probability of finding a loosely bound electron within the capture radius, in sequential spherical shells along the projectile trajectory.

D. Calculations

The electron density of the target $\rho(r)$ is calculated using the Clementi and Roetti[28] tabulated analytic expansion of Roothaan-Hartree-Fock atomic wave functions

$$\rho(r)=\sum_{n,l,m}|\psi_{nlm}(r)|^2 . \tag{14}$$

The target atom is then divided into thin spherical shells so that the probability of an electron being in a given shell is the radial electron density,

$$P(r_i)=4\pi r_i^2\rho(r_i)dr . \tag{15}$$

The thickness dr is taken small enough to give $P(r_i)\ll 1$ for all shells, so unitarity is fulfilled.

As we are integrating the capture probability along the projectile trajectory each spherical shell has an entrance and exit contributions. The probability of capture of an electron from a shell with radius r_i at entrance or exit is proportional to the probability of finding an electron within this shell close enough to the projectile trajectory, i.e., within the capture cylinder, as presented in Fig. 4. This probability is evaluated by integrating the electron density over half of the spherical shell if r_i is smaller than the capture radius, and over a spherical cap (shown in Fig. 4) if r_i is larger than the capture radius. Integrating,

$$P_c(n;r_i)=\int_V\rho(r_i)d\Omega dr = \begin{cases}2\pi h r_i\rho(r_i)dr & \text{if } r_i>R_c(n)\\ 2\pi r_i^2\rho(r_i)dr & \text{if } r_i\le R_c(n)\end{cases} \tag{16}$$

where $h=r_i-[r_i^2-R_c^2(n)]^{1/2}$.

Now, using the definition of the radial electron density [Eq. (15)], the nth-electron capture probability from a shell with radius r_i can be written as a function of radial electron density times a geometric factor:

$$P_c(n;r_i)=\begin{cases}\dfrac{h}{2r_i}P(r_i) & \text{if } r_i>R_c(n)\\ \frac{1}{2}P(r_i) & \text{if } r_i\le R_c(n) .\end{cases} \tag{17}$$

Finally, the probability for n-electron capture is given by integrating the capture probabilities from all spherical shells, $P_{\text{cap}}(n,r_i)$, along the projectile trajectory, i.e., integrating from $-\infty$ to $+\infty$ except the tightly bound electrons confined in a sphere with a radius R_F. The negative r represent the entrance contribution while positive r is the exit contribution, i.e., electron capture before and after the projectile reaches the distance of closest ap-

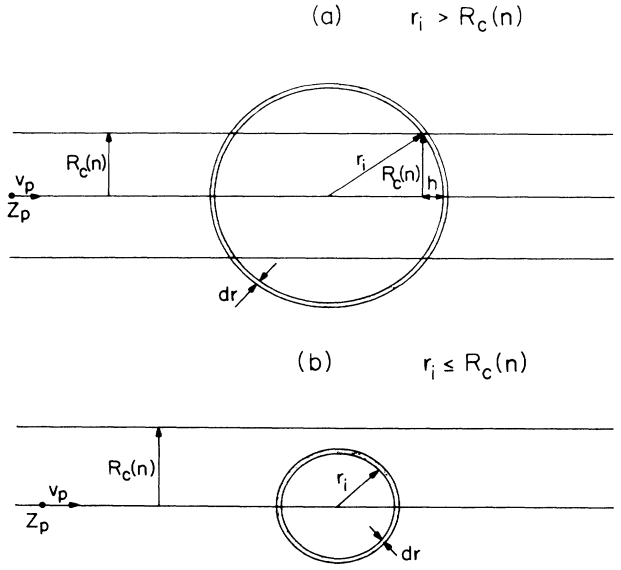

FIG. 4. A schematic view of the probability for capture of an electron from a thin shell with a radius r_i. (a) $r_i>R_c(n)$. (b) $r_i\le R_c(n)$. See text for further details.

proach. The entrance and exit contributions are not the same since capture of an electron at a certain time reduces the chances of capture of an electron later in the collision. Using this Poisson-like process in the evaluation of the capture probabilities as described above ascertains that the unitarity condition will be fulfilled. Thus the probability for capture of n electrons is given by the sum,

$$P_{\rm cap}(n)=\sum_{r_i=-\infty}^{-R_F} P_{\rm cap}(n-1)|_{r_i-dr}P_c(n;r_i)+P_{\rm cap}(n)|_{r_i-dr}[1-P_c(n;r_i)] + \sum_{r_i=+R_F}^{+\infty} P_{\rm cap}(n-1)|_{r_i-dr}P_c(n;r_i)+P_{\rm cap}(n)|_{r_i-dr}[1-P_c(n;r_i)] \quad (18)$$

and the probability for no capture is given by

$$P_{\rm cap}(0)=\sum_{r_i=-\infty}^{-R_F} P_{\rm cap}(0)|_{r_i-dr}[1-P_c(1;r_i)] + \sum_{r_i=+R_F}^{+\infty} P_{\rm cap}(0)|_{r_i-dr}[1-P_c(1;r_i)] \; . \quad (19)$$

IV. RESULTS AND DISCUSSION

The measured single- and double-electron capture probabilities decrease with increasing velocity for the colliding systems under study. This can be seen in Fig. 5 for both Ar and N_2 targets. An attempt to fit these probabilities with a single-electron capture probability using the binomial distribution, commonly used in the independent-electron approximation,[8,26,29] is in disagreement with the experimental results. For example, for $He^{2+}+Ar$ at 400 keV assuming that only the eight M-shell electrons can be captured, we need $P_c(b=0)=0.14$ to get the experimental probability for no capture $P_{\rm cap}(0)=[1-P_c(b=0)]^8=0.29\pm0.02$. With this value for $P_c(b=0)$ the single-electron capture probability $P_{\rm cap}(1)=7P_c(1-P_c)^7=0.39$ underestimates the experimental probability of 0.62 ± 0.02. On the other hand, the double-electron capture probability $P_{\rm cap}(2)=28P_c^2(1-P_c)^6=0.23$ overestimates the experimental probability of 0.13 ± 0.01. This disagreement is most likely a consequence of double-electron capture into states that were autoionized before detection, which is an important relaxation mechanism in He-like systems. This post-collision mechanism will reduce the double-electron probability and will increase the single-electron probability, and is not included in this simple calculation. Thus it is important to include this post-collision autoionization mechanism, at least approximately, in order to compare the calculations to the experimental results.

The outgoing charge state distributions presented in Figs. 6 and 7 were compared to the probabilities predicted by the model of Brandt.[23] For the Ar target we assumed that only M-shell electrons are available for capture. There is a disagreement with the experimental data of about a factor of 2 for high-energy collisions. This deviation increases with decreasing projectile energy. For the N_2 target we assumed that only five outer electrons are available for capture, i.e., the electrons of the other N atom in the molecule are too far to be captured. The agreement with the experimental data is very good for high-energy collisions and about a factor of 2 off at the low-energy collisions. In general, the no-capture channel is underestimated and the double capture channel is overestimated. In the Brandt model capture into autoionizing states is not considered; this may be the major reason for overestimating the double capture. On the other hand, the no-capture channel is a better test of the model as autoionizing states have no contribution to this channel. Thus the disagreement is due to the single-electron capture probability $P_c(b)$ or the statistics used to represent capture from a multielectron target.

The experimental outgoing charge state distributions for the smallest impact parameter measured in each collision system was compared to the "frozen target" model calculation at zero impact parameter. Using this model becomes easier for high velocities, where $v_p^2 \gg 2|\mathcal{E}_T|$; if this condition is fulfilled we can use Eq. (12) to calculate R_c. Our experiments were done with projectile velocities for which only $v_p^2 > 2|\mathcal{E}_T|$ is fulfilled. In this case it is not clear what is the average value of binding energy, $|\mathcal{E}_T|$,

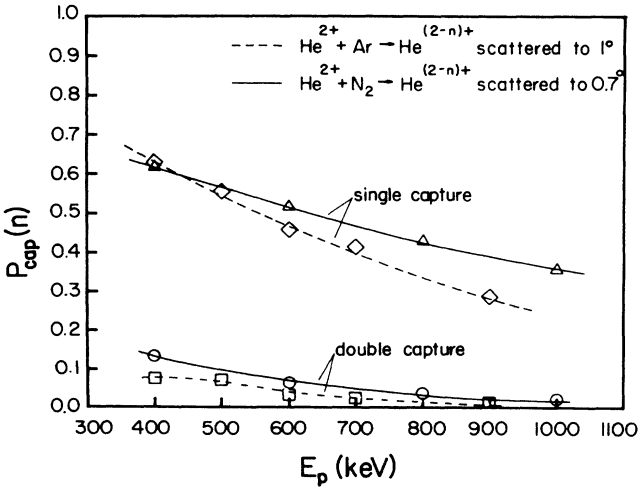

FIG. 5. Single- and double-electron capture probabilities as a function of projectile energy, for $He^{2+}+Ar$ (— — —), and $He^{2+}+N_2$ (——). The lines are drawn to guide the eye.

that should be used in Eq. (11) to evaluate R_c. We used R_c as a single free parameter in the calculation of the outgoing charge state distributions of the He. This calculation is compared with the experimental results of $He^{2+}+Ar$ at different projectile energies in Fig. 6. The agreement between the experiment and the calculation improves as the velocity of the projectile increases. Similar results for the $He^{2+}+N_2$ are given in Fig. 7. The calculations were done assuming that in the close collision electrons are captured mainly from one atom in the molecule and using atomic nitrogen wave functions. Again the agreement between the model and experiment is quite good and improves with increased projectile velocity. The capture radius used for each fitting is mentioned in the figures. The numerical integration convergence was tested by varying the integration limits and the step size.

The average binding energy of the target is expected to increase with increasing projectile velocity as the contribution of electrons having larger orbital velocity increases. However, in the velocity range that the experiments were performed this change is expected to be very small. In order to test the validity of our model we assumed that the average binding energy $|\mathcal{E}_T|$ is constant for all projectile energies. In Fig. 8 we show the dependence of Z_p/R_c on the projectile energy $V_p^2/2$. If Eq. (11) holds and $|\mathcal{E}_T|$ is approximately constant we expect the following linear dependence:

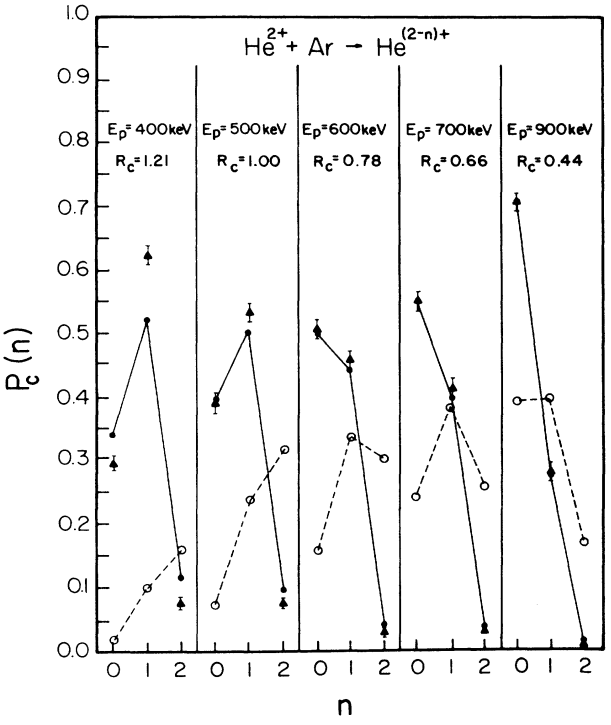

FIG. 6. Outgoing charge state distributions of He^{2+} projectiles scattered on Ar target at different projectile energies. "Frozen target" model —●—, R_c is the capture radius used in this calculation at each energy. Brandt model — — —○— — —. The experimental results are represented by closed triangles, ▲.

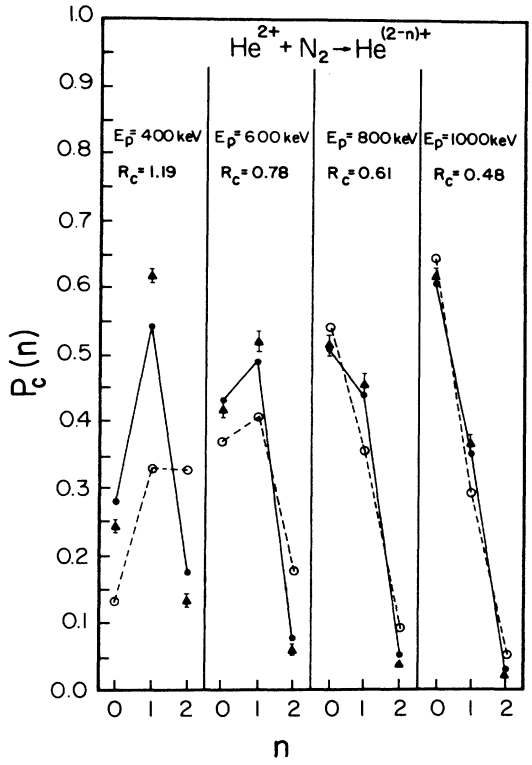

FIG. 7. Outgoing charge state distributions of He^{2+} projectiles scattered on N_2 target at different projectile energies. "Frozen target" model —●—, R_c is the capture radius used in this calculation at each energy. Brandt model — — —○— — —. The experimental results are represented by closed triangles, ▲.

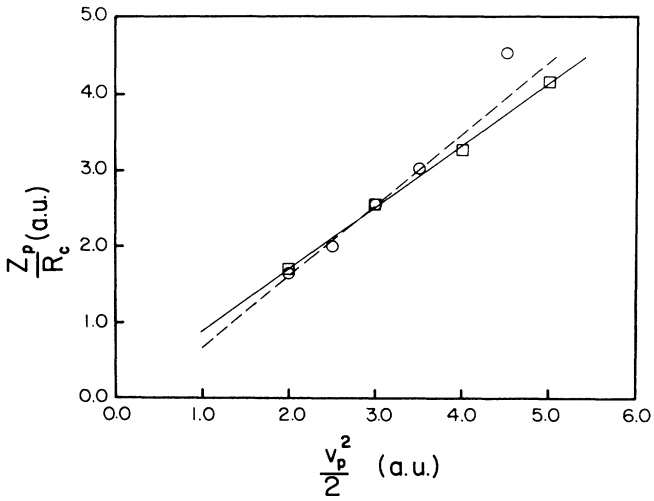

FIG. 8. Z_p/R_c as a function of projectile energy $v_p^2/2$. Ar target, — — —○— — —; N_2 target, ——□——. The lines are the best linear fit of the expression given in Eq. (20).

$$\frac{Z_p}{R_c}=\frac{v_p^2}{2}-|\mathcal{E}_T| \ . \tag{20}$$

It is clearly seen that the capture radius fitted to the data follows the expected linear relation. The deviation from the straight line for He^2+Ar at 900 keV can be caused by an increase in the average binding energy as the $3s$ Ar orbital ($v_{3s}\sim 4.5$ a.u.) starts to contribute. The average binding energy of the loosely bound electrons is given by the intersection of the linear fit presented in Fig. 8 and is approximately zero for the N_2 target and about 0.25 a.u. for the Ar target. Thus, in these collisions the capture radius can be approximated by the simple expression given in Eq. (12), i.e., $R_c=2Z_p/v_p^2$.

V. CONCLUSIONS

Outgoing charge state distributions of He^{2+} after a single close collision with Ar and N_2, at 400–1000 keV, were presented. These charge state distributions are almost independent of the impact parameter for small impact parameters. The probability for double-electron capture for these collisions is relatively large, of the order of few percent, and increases with decreasing velocity. A "frozen target" model was developed based on the classical Bohr-Lindhard electron capture model. In this model special attention was given to fulfill unitarity and to account for post-collision autoionization that causes a decrease in the detected double-electron capture and a concurrent increase in the single-electron capture. This model is easy to use and is in good agreement with the measured single- and double-electron capture probabilities at small impact parameters.

ACKNOWLEDGMENTS

We thank Mr. J. Saban for his invaluable technical assistance. This research was supported by the Foundation for Promotion of Research at the Technion, and by Technion Vice President Research Fund–Morantz Energy Research Fund.

*Present address: Department of Physics, Kansas State University, Manhattan, KS 66506.

†Present address: Brookhaven National Laboratory, Upton, NY 77843

[1]T. V. Goffe, M. B. Shah, and H. B. Gilbody, J. Phys. B **12**, 3763 (1979).

[2]J. R. Macdonald and F. W. Martin, Phys. Rev. A **4**, 1965 (1971).

[3]T. R. Dillingham, J. R. Macdonald, and P. Richard, Phys. Rev. A **24**, 1237 (1981).

[4]H. Damsgaard, H. K. Haugen, P. Hvelplund, and H. Knudsen, Phys. Rev. A **27**, 112 (1983).

[5]R. Hippler, S. Datz, P. D. Miller, P. L. Pepmiller, and P. F. Dittner, Phys. Rev. A **35**, 585 (1987).

[6]S. Datz, R. Hippler, L. H. Andersen, P. F. Dittner, H. Knudsen, H. F. Krause, P. D. Miller, P. L. Pepmiller, T. M. Rosseel, N. Stolterfoht, Y. Yamazaki, and C. R. Vane, Nucl. Instrum. Methods **A262**, 62 (1987).

[7]P. Richard, J. Hall, J. L. Shinpaugh, J. M. Sanders, T. N. Tipping, T. J. M. Zouros, D. H. Lee, and H. Schmidt-Bocking, Nucl. Instrum. Methods, **A262**, 69 (1987).

[8]W. E. Meyerhof, R. Anholt, Xiang-Yuan Xu, H. Gould, B. Felsberg, R. J. McDonald, H. E. Wegner, and P. Thieberger, Nucl. Instrum. Methods **A262**, 10 (1987).

[9]Dz. Belkic, R. Gayet, and A. Salin, Phys. Rep. **56**, 281 (1979).

[10]J. Alonso, P. Thieberger, and H. E. Wegner, Phys. Rev. A **32**, 3291 (1985).

[11]H. C. Brinkman and H. A. Kramers, Proc. Acad. Sci. Amsterdam **33**, 973 (1930).

[12]B. Rosner and D. Gur, Phys. Rev. A **15**, 70 (1977).

[13]M. Meron, D. Maor, and B. Rosner, J. Phys. B **16**, 3983 (1983).

[14]M. Meron and B. Rosner, Phys. Rev. A **30**, 132 (1984).

[15]B. Rosner, D. W. Mingay, and E. Barnard, S. Afr. J. **6**, 1 (1983).

[16]E. Horsdal-Pedersen, C. L. Cocke, and M. Stockli, Phys. Rev. Lett. **50**, 1910 (1983).

[17]H. Vogt, R. Schuch, E. Justiniano, M. Schulz, and W. Schwab, Phys. Rev. Lett. **57**, 2256 (1986).

[18]E. Horsdal-Pedersen, J. Phys. B **20**, 785 (1987).

[19]L. H. Thomas, Proc. R. Soc. London Ser. A **114** (1927).

[20]N. Bohr, K. Dan. Vidensk. Selsk. Mat.-Fys. Medd. **18** (8) (1948).

[21]N. Bohr and J. Lindhard, K. Dan. Vidensk. Selsk. Mat.-Fys. Medd. **28** (7) (1954).

[22]H. Knudsen, H. K. Haugen and P. Hvelplund, Phys. Rev. A **23**, 597 (1981).

[23]D. Brandt, Nucl. Instrum. Methods **214**, 93 (1983).

[24]U. Fano and W. Lichten, Phys. Rev. Lett. **14**, 627 (1965).

[25]M. Meron, D. Maor, and B. Rosner, Phys. Lett. **74A**, 201 (1979).

[26]R. E. Olson, J. Phys. B **11**, 1843 (1979).

[27]D. Zajfman and D. Maor, Phys. Rev. Lett. **56**, 320 (1986).

[28]E. Clementi and C. Roetti, At. Data Nucl. Data Tables **14**, 177 (1974).

[29]J. H. McGuire and O. L. Weaver, Phys. Rev. A **16**, 41 (1977).